Removal of Uranium (VI) with Iron Nanoparticles

Julieta Crespi[a], Natalia Quici[b], Emilia B. Halac[c], Ana G. Leyva[c], Cinthia P. Ramos[b,c], Martín Mizrahi[b,d], Félix G. Requejo[b,d] and Marta I. Litter*[b,c]

[a]Instituto Sábato, Comisión Nacional de Energía Atómica, Universidad Nacional de Gral. San Martín, Av. Gral. Paz 1499, 1650 San Martín, Prov. de Buenos Aires, Argentina
[b]Consejo Nacional de Investigaciones Científicas y Técnicas, Av. Rivadavia 1917, 1033 Ciudad Autónoma de Buenos Aires, Argentina
[c]Comisión Nacional de Energía Atómica, Av. Gral. Paz 1499, 1650 San Martín, Prov. de Buenos Aires, Argentina
[d]Instituto de Investigaciones Fisicoquímicas Teóricas y Aplicadas, Facultad de Ciencias Exactas, Universidad Nacional de La Plata, Diag. 113 y 64, 1900 La Plata, Argentina
litter@cnea.gov.ar, marta.litter@gmail.com

In this work, the removal efficiency of U(VI) from water using commercial nanoparticles of zerovalent iron (nZVI) (NANOFER 25, NANO IRON s.r.o.) and magnetite (nM) (NanoFe®, Nanotek SA) was evaluated. Batch experiments were carried out in a jacketed reactor with a vertical paddle stirrer, using $UO_2(NO_3)_2$ solutions ($[U(VI)]_0 = 0.25$ mM $\equiv 59.5$ mg L^{-1}) at pH 5.3. The nanoparticles (initially suspended in water) were added to the U(VI) solution to achieve different Fe:U(VI) molar ratios (MR) in the range of 1 to 100. U(VI) removal with nZVI and nM at MR 4 and dissolved oxygen (DO) levels higher than 0.1 mg L^{-1} were rather efficient, reaching in both cases a final removal of 65 %. Under these conditions, uranium removal strongly depends on the presence of DO, decreasing with increasing DO. When 40 and 100 MR were used, a complete U(VI) removal in the first 15 min of treatment was observed, and oxygen was consumed reaching negligible DO levels (below 0.1 mg L^{-1}). With MR = 4 and DO levels below 0.1 mg L^{-1} (achieved by N_2 bubbling), removal of U(VI) was complete in 60 min of reaction for both types of nanoparticles. Although the trend of the removal curves was similar, the advantage of nM is that very low levels of iron in solution (as Fe(total)), below 1 mg L^{-1}, were observed during the whole reaction time, while it was 5 mg L^{-1} for nZVI at the end of the run, mainly as Fe(II). Analysis of the final solids by XANES and Raman spectroscopies revealed the presence of uranium, probably as UO_2.

1. Introduction

The most common form of uranium in aqueous phase is uranyl ion, UO_2^{2+}. Uranium levels can reach 50 mg L^{-1} in certain natural groundwaters, which may derive in significant concentrations in drinking water (Noubactep et al. 2006). Additional anthropic contamination sources are lixiviation of deposits, mining tailings, nuclear industry emissions, coal combustion, etc. Conventional water treatment processes can be a partial or insufficient solution for uranyl removal due to low efficiency or high associated costs. In these cases, advanced reduction processes based on the use of iron nanoestructurated materials like nanozerovalent iron (nZVI) or nanomagnetite (nM) are a good alternative. The importance of these materials lies in their ability to combine chemical transformation with adsorption and coprecipitation processes on the surface of the contaminants, being able to remove even traces of the contaminant.

Some authors (Crane & Scott 2014) have shown that the corrosion lifespan and associated U(VI) removal efficacy of nanoscale zerovalent iron is enhanced in the absence of dissolved oxygen (DO). Additionally, the use of high Fe:U molar ratios leads to DO values lower than 0.1 mg L^{-1}, reaching, at the same time, high uranium removal percentages (Crane et al. 2011).

2. Materials and methods

2.1 Chemicals

U(VI) solutions were prepared using $UO_2(NO_3)_2.6H_2O$ provided by May & Baker (now Sanofi-Aventis). Commercial nZVI (NANOFER 25, hereafter nZVI) was provided by NANOIRON s.r.o. (Czech Republic) as a suspension with [Fe(total)] = 242 g L^{-1} and 80-85 g Fe(0)/100 g Fe(total). Commercial nM (NanoFe®, hereafter nM) was provided by Nanotek S.A. (Argentina) as a suspension with [Fe(total)] = 25.9 g L^{-1}. Both suspensions were kept at low temperature (~ 4 °C) until used. o-phenanthroline (Mallinckrodt), HNO_3 (Biopack), hydroquinone (Merck), 4-(2-pyridylazo)resorcinol monosodium salt monohydrate (PAR) (Merck), triethanolamine (TEA) (Biopack),NaOH (Biopack) were of analytical reagent grade and used without further purification. In all experiments, Milli-Q water was used (resistivity = 18 MΩ cm). Nitrogen (purity 5.0) was provided by Linde.

2.2 Experimental setup

Batch experiments were carried out in a 400 mL cylindrical jacketed Pyrex glass reactor closed to the atmosphere by means of a gas tight lid. Temperature was controlled by recirculating water through the jacket using a Polystat® temperature controller (Cole-Parmer), and the suspension was stirred by a vertical paddle agitator (Decalab). Nitrogen was bubbled constantly in the reactor through a glass tube provided with a fritted glass at the bottom in order to ensure anoxic conditions. All experiments were performed using 200 mL of 0.25 mM U(VI) solution. The procedure for the preparation of the suspensions included the addition of an aliquot of the original concentrated suspension of nZVI or nM in N_2 purged water followed by the homogenization during 5 min and the addition of the uranium solution. The efficiency of nZVI was evaluated using MRs in the range of 1 to 100 (the molarity of nZVI or nM is expressed as Fe(total)) and MR = 4 in the case of nM. pH was adjusted to 5.3 using dilute HNO_3 (20 %) or NaOH (1 or 4 M).

2.3 Analytical methods

Samples (1.2 mL) were periodically withdrawn and centrifuged in Eppendorf tubes during 2 min using an Eppendorf MiniSpin centrifuge at 13,000 rpm. The supernatant of each sample was used separately to determine U(VI), U(total), Fe(II) and Fe(total). [U(VI)] was measured spectrophotometrically using the PAR method at 530 nm (Florence & Farrar 1963). [Fe(II)] and [Fe(total)] were measured spectrophotometrically using the o-phenanthroline method at 508 nm (Bandemer & Schaible 1944). UV-Vis absorption measurements were performed employing a Hewlett Packard Agilent 8453UV-Vis spectrophotometer. [U(total)] in solution was measured employing Total Reflection X-ray Fluorescence (TXRF) using [Ga] = 1 mg L^{-1} as internal standard. An S2 PICOFOX (Bruker) spectrometer, automatic version, was used for TXRF measurements.

Initial and final pH determinations were carried out using a pH-meter (Meterlab PH M210), and dissolved O_2 was measured with an oxygen sensor (Hach Sens Ion 156 Multiparameter Meter) equipped with a Hach DO meter electrode. All experiments were performed at 23 ± 1 °C at least by duplicate, and the results averaged.

2.4 Characterization of the solids

X-ray diffraction (XRD), Raman, Mössbauer and XANES (X-ray absorption near edge spectroscopy) analyses were carried out to characterize the iron nanoparticles before and after exposure to U(VI). After the treatment, the solid particles were filtered using 0.22 μm nylon membranes (Osmonics), and preserved under vacuum before analysis.

Raman spectra were recorded on a LabRAM HR Raman system (Horiba Jobin Yvon), equipped with two monochromator gratings and a charge coupled device detector. The He-Ne laser line at 632.8 nm was used as excitation source. The laser fluence was adjusted to ensure the minimization of the heating so that the sample was not altered.

Mössbauer data were recorded at 10 mm/s and room temperature using a conventional constant acceleration spectrometer in transmission geometry with a ^{57}Co/Rh source. The obtained spectrum was then fitted using the Normos program developed by Brand (1991).

XRD patterns were obtained with a PanAnalytical Empirean X-ray diffractometer with PIXcel 3D detector, using Cu-Kα radiation, over a range in 2θ of 10 to 100° with step of 0.026° and 24 seconds by step.

XANES analyses were performed using the in-house X-ray absorption spectrometer, Rigaku R-XAS Looper. U L_3-edge (E_0 = 17,166 eV) X-ray XANES spectra was measured at room temperature in the transmission mode. XAS spectra were collected from 17,070 to 17,400 eV in reduced steps of 0.6 eV in the XANES region. Data were processed using *ATHENA* with the *AUTOBK* background removal algorithm (Ravel & Newville, 2005). The spectra were pre- and post-edge normalized to obtain an edge jump of unity to facilitate comparisons across different samples. The spectrometer was calibrated in energy using an yttrium reference sample (E_0 = 17,038 eV) measured in the same conditions as the samples.

BET (Brunauer-Emmett-Teller) specific surface area of the nanoparticles was measured by N_2 adsorption-desorption isotherm at 77 K using a Micromeritics ASAP® 2420 Accelerated Surface Area and Porosimetry System (Micromeritics Instrument Corp., Norcross, GA).

3. Results and discussion

3.1 Characterization of the initial iron nanoparticles

In this work, the zerovalent iron nanoparticles provided by NANOIRON s.r.o. were only analyzed by Raman spectroscopy as the material was extensively characterized before. According to the supplier, the suspension of nanoparticles are composed by 14-18 % Fe(0) and 2-6 % Fe_3O_4 with a BET area of 20-25 m^2 g^{-1} and a particle size between 50 and 65 nm (NANOIRON s.r.o. 2008-2010). These features were confirmed by SEM and XRD results, and a core-shell like structure with a Fe(0)-rich core surrounded by a magnetite-rich shell was proposed by our group based on XPS analysis, which showed that the external layer is exclusively composed of mixed iron oxides (mainly magnetite), with a decreasing Fe(II) gradient towards the core of the nanoparticle (Montesinos et al. 2014).

In the present work, Raman spectra were acquired to confirm the structure of nZVI (Figure 1a). As can be observed, the results indicate that both magnetite and hematite might be present in the material.

In the case of nM, BET determination indicated a surface area of 48.75 m^2 g^{-1}. Raman and Mössbauer spectroscopies and XRD results are shown in Figure 1. The presence of magnetite was confirmed by the three techniques. Mössbauer and Raman spectra indicated that maghemite could be also present in the sample, without evidence of the presence of Fe(0).
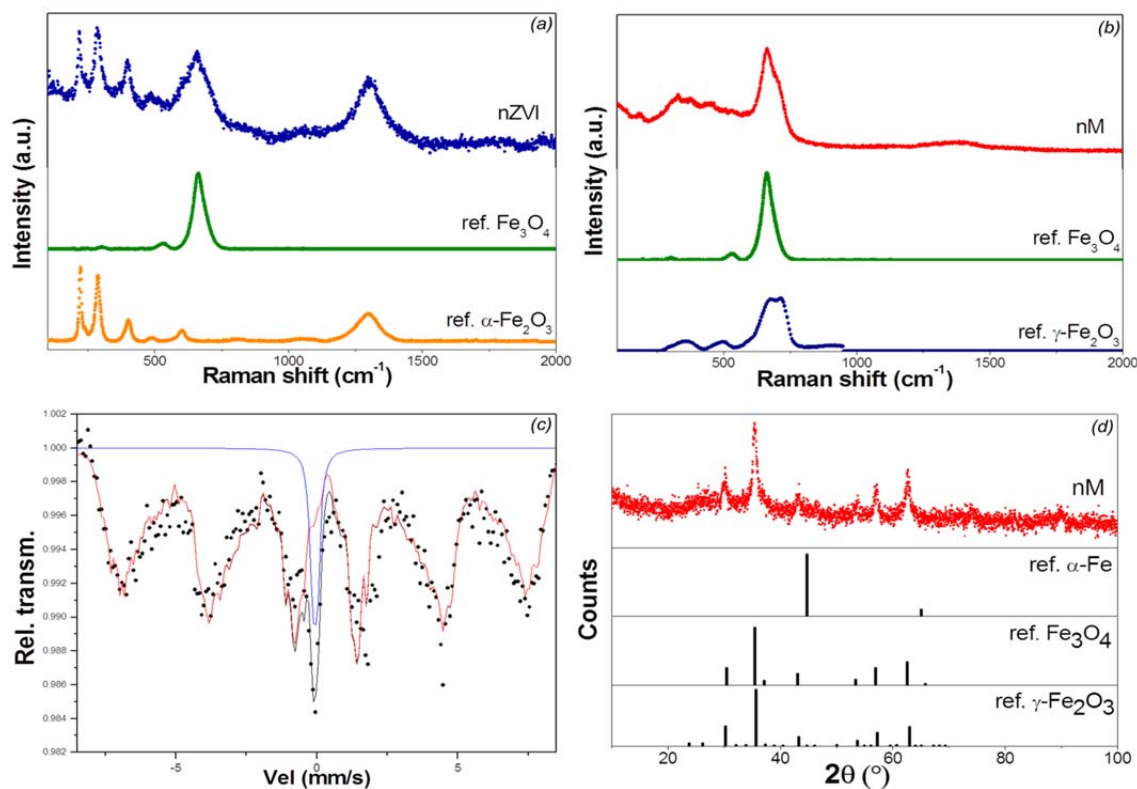
Figure 1: (a) Raman spectrum for nZVI. Spectra for hematite and magnetite provided by RRUFF database, (Lafuente et al. 2015) are also shown for comparison; (b) Raman spectrum for nM. Spectra of maghemite and magnetite provided by RRUFF Database (Lafuente et al. 2015) are also shown for comparison; (c) Mössbauer spectrum for nM; (d) XRD pattern for nM particles. Magnetite, maghemite and α-Fe reference peaks are shown.

The results of the characterizations for both materials are summarized in Table 1.

Table 1: nZVI and nM characterization results

	Particle size (nm)	[Fe^0] (g Fe^0/100 g Fe(total))	BET area surface (m^2 g^{-1})	Oxides present in the sample
nZVI	50-65[a,b]	80-85[a]	20-25[a]	Fe$_3$O$_4$[a,b,c],α-Fe$_2$O$_3$[c]
nM		0[c]	48.75[c]	Fe$_3$O$_4$[c], γ-Fe$_2$O$_3$[c]

a. Data from (NANOIRON s.r.o. 2008-2010); b. Data from (Montesinos et al. 2014); c. This work.

3.2 Experiments of U(VI) removal: effect of the Fe:U MR

As can be observed in Figure 2a, 50 % of the initial U(VI) concentration was removed with MR = 1 at 120 min, and a fast (60 min) and complete removal was obtained with MR = 4. Two higher MRs were also tested (40 and 100), which yielded 100 % removal in 15 min (results for MR = 100 are not shown). As the MR increases, the release of iron to solution also increases, mainly as Fe(II) (Figure 2b). The iron concentration developed in solution at MR = 40 reached 100 mg L^{-1} at the end of the run; in the case of the lower MRs, the iron concentration remained around 5 mg L^{-1} after the first hour of reaction.

In the case of nM (Figure 3a), the trend of removal curves is similar to those with nZVI. Remarkably, under the same conditions (MR = 4, DO < 0.1 mg L^{-1}), much lower amounts of Fe were released to the solution when using nM compared with nZVI, the iron concentration remaining below 1 mg L^{-1} during the whole reaction time (Figure 3b).

3.3 Experiments of U(VI) removal: effect of DO

Figure 4 shows the effect of DO in the removal of uranium for MR = 4. As previously indicated by other authors (Crane et al. 2011), a level of DO higher than 0.1 mg L^{-1} considerably reduces the removal capability of the system: after 120 min, only 65 % removal was obtained with DO > 0.1 mg L^{-1} in comparison with more than 90 % removal for DO < 0.1 mg L^{-1}, for both samples.

3.4 XRD, XANES and Raman analysis of the solids after reaction with U(VI)

The XRD analysis of the solid obtained after 120 min of contact of nZVI with the U(VI) solution indicated the presence of magnetite or maghemite and the absence of Fe(0) (Figure 5a), in contrast with the initial material (see 3.1). Raman analysis suggested the presence of uranium oxides, and a more specific analysis provided by XANES confirms the formation of some U(IV) compound, probably UO$_2$ (Figure 5b). Raman analysis of solids obtained after U(VI) removal using nM, indicated the presence of magnetite and maghemite (Figure 6a), as in the initial material (see 3.1); the peak of maghemite is more clearly observed here. The presence of uranium mostly in (IV) oxidation state, as in the case of nZVI, was confirmed by XANES (Figure 6b).
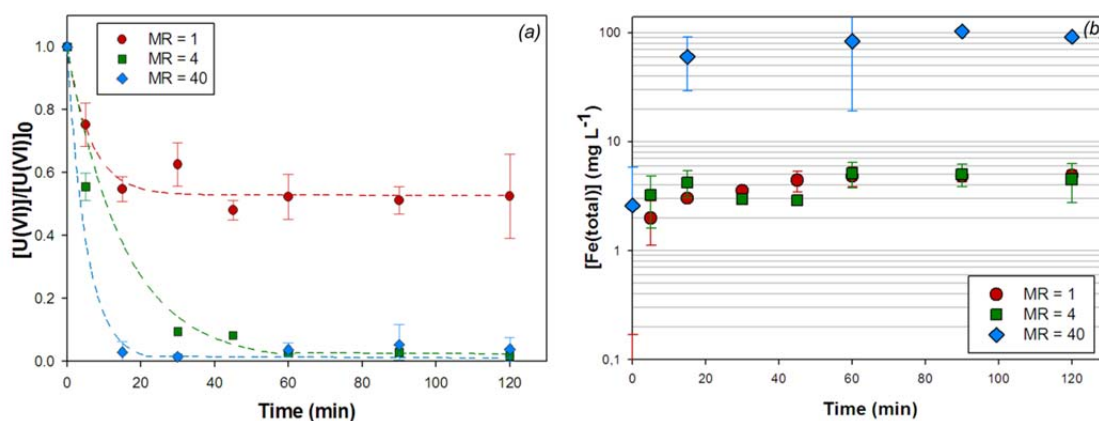
Figure 2: (a) Removal of uranium with nZVI at different Fe:UMRs, [U(VI)]$_0$= 0.25 mM, initial pH 5.3, T = 23 ± 1 °C, DO < 0.1 mg L^{-1}. Dashed curves are only for a better visualization of points and do not correspond to any fitting model; (b) Y-axis semi-log plot for the evolution of [Fe(total)] in each experiment.
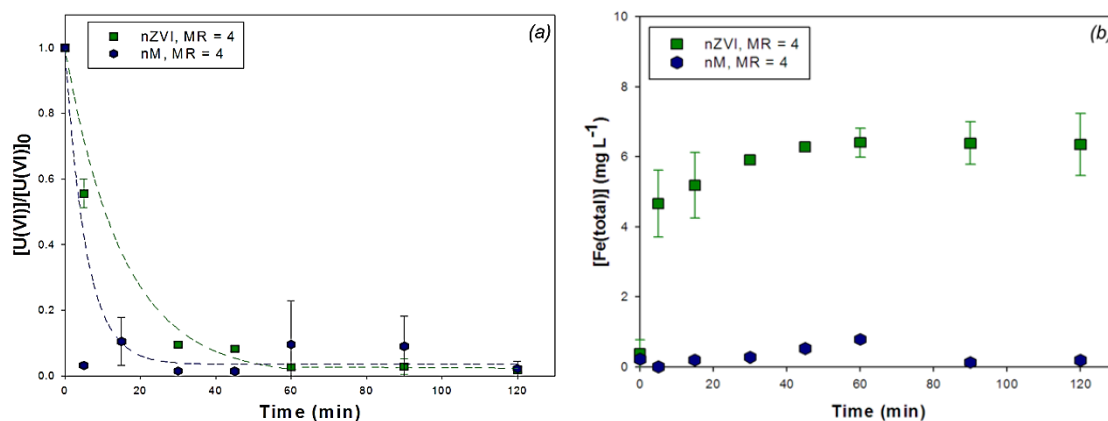
Figure 3: (a) Comparison between U(VI) removal with nZVI and nM, at MR = 4. $[U(VI)]_0$= 0.25 mM, initial pH 5.3, T = 23 ± 1 °C, anoxic (DO < 0.1 mg L^{-1}). Dashed curves are only for a better visualization of points and do not correspond to any fitting model; (b) evolution of [Fe(total)] in experiments with nM and nZVI under the same conditions.
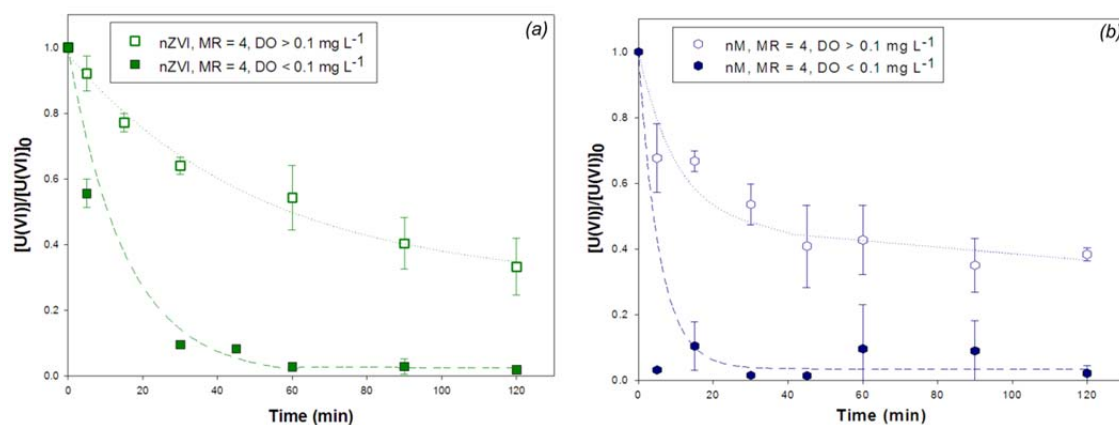
Figure 4: (a) Removal of U(VI) with nZVI at Fe:U MR = 4, with DO < 0.1 mg L^{-1} and DO > 0.1 mg L^{-1}; (b) removal of U(VI) with nM at MR Fe:U = 4, with DO < 0.1 mg L^{-1} and DO > 0.1 mg L^{-1}. $[U(VI)]_0$= 0.25 mM, initial pH 5.3, T = 23 ± 1 °C. Dashed curves are only for a better visualization of points and do not correspond to any fitting model.
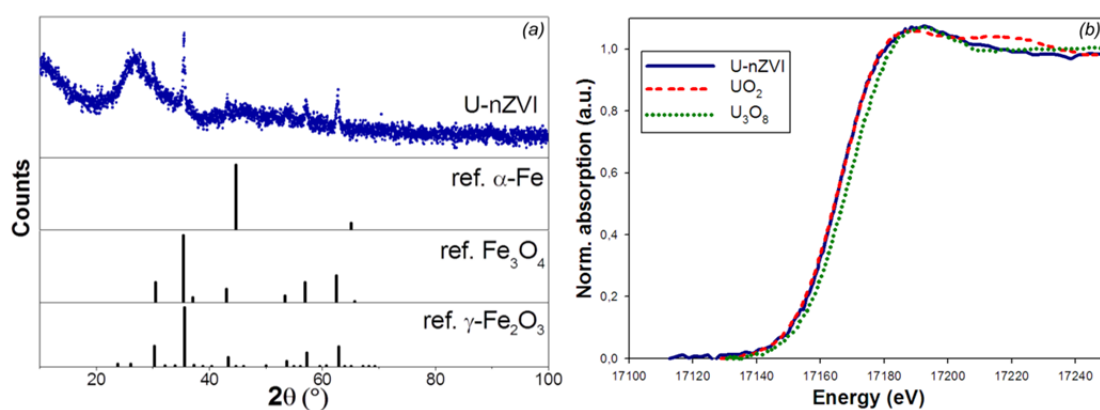
Figure 5: (a) XRD pattern of the solid obtained after removal of U(VI) with nZVI. Spectra of magnetite and maghemite are also shown for comparison. Amorphous signals correspond to the filter used to remove the particles (section 2.4); (b) XANES spectrum of the solid obtained after removal of U(VI) with nZVI. Spectra of UO_2 and U_3O_8 are also shown for comparison.
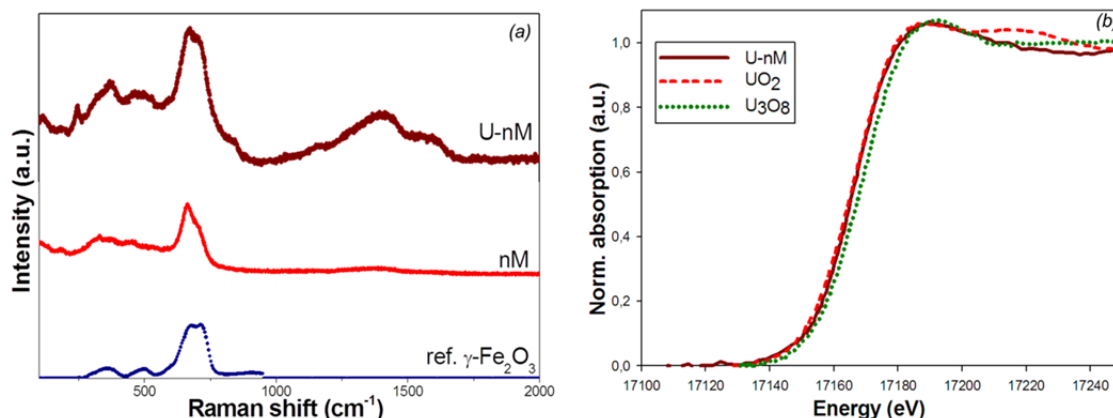
Figure 6: (a) Raman spectra of the solids obtained after U(VI) removal with nM (U-nM), nM before treatment, and maghemite reference; (b) XANES spectrum of the solid obtained after U(VI) removal with nM. Spectra of UO$_2$ and U$_3$O$_8$ are also shown for comparison.

4. Conclusions

Under the present experimental conditions, both commercial nZVI and nM showed to be efficient for U(VI) removal from water. Low levels of DO are crucial in order to achieve high U(VI) removal percentages (100 % vs. 65 % for the MR = 4 compared here). At the same time, the need of near anoxic conditions makes the technology promising for its use for remediation of soils and groundwater. The use of nM leaves a lesser amount of Fe in solution compared with nZVI, in the first case very close to the limit set by the Argentine Food Code for drinking water (0.3 mg L^{-1}). Additionally, for a near future pilot or real scale application in our country, the use of nM would be more convenient as this is an Argentine national product.

References

Bandemer S.L., Schaible P.J., 1944, Determination of iron: A study of the o-phenanthroline method, Ind. Eng. Chem. 16, 317-319.

Brand R.A., 1991, Normos Programs (SITE-DIST), Duisburg University.

Crane R.A., Dickinson M., Popescu J.C., Scott T.B., 2011, Magnetite and zero-valent iron nanoparticles for the remediation of uranium contaminated environmental water, Water Res 45(9), 2931-2942.

Crane R.A., Scott T.B., 2013, The effect of vacuum annealing of magnetite and zero-valent iron nanoparticles on the removal of aqueous uranium, J. Nanotechnol. 2013.

Crane R.A., Scott T.B., 2014, The removal of uranium onto nanoscale zero-valent iron particles in anoxic batch systems, J. Nanomater. 2014.

Florence T.M., Farrar Y., 1963, Spectrophotometric determination of uranium with 4-(2-Pyridylazo)resorcinol, Anal. Chem. 35(11),1613-1616.

Lafuente B., Downs R.T., Yang H., Stone N., 2015, The power of databases: the RRUFF project. In: Highlights in Mineralogical Crystallography, Eds. Armbruster T., Danisi R.M., Berlin, Germany, W. De Gruyter, 1-30.

Montesinos V.N., Quici N., Halac E.B., Leyva A.G., Custo G., Bengio S., Zampieri G., Litter M.I., 2014, Highly efficient removal of Cr(VI) from water with nanoparticulated zerovalent iron: Understanding the Fe(III)-Cr(III) passive outer layer structure, Chem. Eng. J. 244, 569-575.

NANOIRON s.r.o., 2008-2010, NANOIRON Future Technology <nanoiron.cz> accessed 16.10.2015.

Noubactep C., Schöner A., Meinrat G., 2006, Mechanism of uranium removal from the aqueous solution by elemental iron, J. Hazard. Mater. 132(2-3), 202-212.

Ravel B., Newville M., 2005, ATHENA, ARTEMIS, HEPHAESTUS: data analysis for X-ray absorption spectroscopy using IFEFFIT, J. Synchrotron Rad. 12, 537-541.